Surface Science 664 (2017) 70–75

Contents lists available at ScienceDirect

Surface Science

journal homepage: www.elsevier.com/locate/susc

1D chain formation by coadsorption of Pb and Bi on Cu(001): Determination using low energy electron diffraction

Md Kabiruzzaman*, Rezwan Ahmed, Takeshi Nakagawa, Seigi Mizuno

Interdisciplinary Graduate School of Engineering Science, Kyushu University, Kasugashi, Kasugakoen, 6-1, Fukuoka 8168580, Japan

ARTICLE INFO

Keywords:
Coadsorption
Heavy metals
Pb
Bi
Cu(001)
Low energy electron diffraction
1D arrangement
Surface structure
Morphology
Roughness
Topology
Surface alloy

ABSTRACT

Coadsorption of two heavy metals, Pb and Bi, on Cu(001) at room temperature has been studied using low energy electron diffraction (LEED). $c(4\times4)$, $c(2\times2)$, and $c(9\sqrt{2}\times\sqrt{2})$ phases are obtained at different coverages; here, we have determined the best-fit structure of $c(4\times4)$ phase. This structure can be described as a 1D substitutional chain arrangement of Pb and Bi atoms between the Cu rows along the [110] direction. The unit cell in the two-dimensional (2D) surface consists of one Bi atom, two Pb atoms, and four Cu atoms with one vacancy at the center. The optimal structure parameters demonstrate that Bi atoms are located at fourfold-hollow sites and that Pb atoms are laterally displaced by 0.78 Å from the fourfold-hollow site toward the vacancy. The reasons for the formation of the $c(4\times4)$ structure upon deposition of Pb and Bi on Cu(001) are discussed in comparison with a similar structure formed by the individual adsorption of Pb on the same substrate.

1. Introduction

Novel two-dimensional (2D) surface materials have attracted great interest because of their specific structure, composition, and properties, which differ from those of the bulk [1–2]. These 2D materials can consist of a single element like graphene [3], silicene [4], or germanene [5], or two elements like MoS_2 or WSe_2 [6]. Besides these monoatomic or diatomic 2D materials, there is now also emphasis upon forming 2D materials with three elements. These types of materials are currently studied for applications in microelectronics, catalysis, surface-energy gaining and so forth. The materials having three elements, sometimes termed ternary alloys, can be grown on both metal and semiconductor substrates. Some examples of ternary alloys grown on semiconductors are Pb and Tl on Si(111) [7], Pb and Sn on Si(111) [8], Bi and Sb on Si(111) [9] and Sn and Ag on Ge(111) [10]. Some examples of metal substrates are Pb and Sn on Rh(111) [11], Mg and Bi on Cu(001) [12], and Bi and Mn on Cu(001) [13].

With regard to metals on a metal surface, heavy metals like Pb and Bi individually show interesting properties on Cu(001). Both elements show alloy structures at lower coverages (<0.5) [13–15], whereas at higher coverages (≥0.5), they form overlayer structures [15–17], as shown in Fig. 1. The coverage is defined as the ratio of the number of adsorbate atoms to the number of substrate atoms located in the 2D (1×1) unit cell. In the case of Pb, a $c(4\times4)$ substitutional alloy structure is shown at the coverage of 0.375 [14], becoming a $c(2\times2)$ [16] overlayer structure at a coverage of 0.5. In the case of Bi, $p(2\times2)$ [15] and $c(4\times2)$ [13] are both substitutional structures formed at coverages of 0.25 and 0.375, respectively, whereas they become overlayer structures at 0.5 [15]. Although Pb and Bi are larger than Cu by 37% and 33%, respectively in the pure 3D bulk values, they form different substitutional structures on the surface of Cu(001), as mentioned above. It is our intention to study the behaviors of Pb and Bi, during coadsorption of these two atoms onto a Cu(001) substrate. Upon coadsorption, we obtained $c(4\times4)$, $c(2\times2)$, $c(9\sqrt{2}\times\sqrt{2})$. The $c(2\times2)$ phase was determined previously [17], and it was shown that phase separation or mixture of individual $c(2\times2)$ phases of Pb and Bi occurs and the elements do not mix with each other on the surface.

In this study, we determine the structure of the Pb and Bi coadsorbed $c(4\times4)$ phase. Before doing so, we determine the $c(4\times4)$ phase of individual adsorption of Pb onto Cu(001) more accurately than in the previous report [14]. We reconfirm the 1D chain of Pb atoms between the Cu rows in the [110] direction and obtain a similar 1D chain arrangement for Pb and Bi coadsorption. The details of this structure and the comparison of the different parameters of this $c(4\times4)$ phase of coadsorption with the corresponding phase of the individual Pb case are described here.

---

* Corresponding author.
E-mail address: kabir.apece@gmail.com (M. Kabiruzzaman).

http://dx.doi.org/10.1016/j.susc.2017.05.017
Received 6 May 2017; Received in revised form 31 May 2017; Accepted 31 May 2017

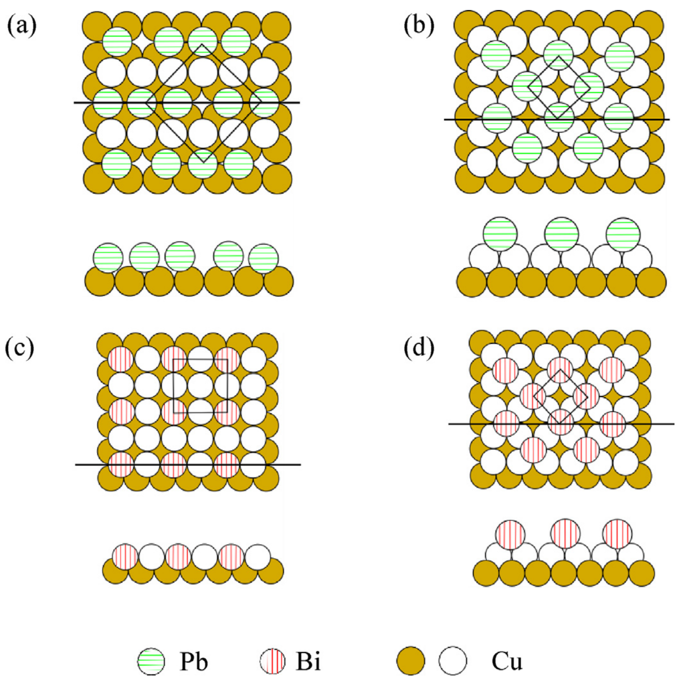

Fig. 1. Top and cross-sectional views (perpendicular to the line drawn) of the (a) Cu(001)-$c(4\times4)$-3Pb, (b) Cu(001)-$c(2\times2)$-Pb, (c) Cu(001)-$p(2\times2)$-Bi, and (d) Cu(001)-$c(2\times2)$-Bi phases, which are obtained at the coverages of 0.375, 0.5, 0.25, and 0.5, respectively. Models (a) and (c) have substitutional structures, and models (b) and (d) have overlayer structures. Unit cells are outlined.

2. Experiment

Experiments were performed in an ultrahigh vacuum (UHV) chamber equipped with a four-grid LEED system. The base pressure of the UHV chamber was approximately 5×10^{-8} Pa. To clean the Cu(001) surface, we used several cycles of Ar^+ sputtering (1 kV, 6.5 μA, 15 min) and subsequent annealing until a sharp (1×1) LEED pattern was obtained. When the sample reached room temperature, Pb and Bi were deposited by heating with different sources. After deposition, we used liquid N_2 to cool the sample. At a temperature of 120 K, the LEED-beam spots were measured using a digital charge-coupled-device camera with a computer-controlled data-acquisition system [19]. Incident energy ranges of 50–500 and 100–500 eV were used to obtain the $I(E)$ curves of the LEED beams of the individual and coadsorption cases, respectively. Barbieri/Van Hove symmetrized automated tensor LEED package was used to calculate the theoretical $I(E)$ curves for structure models to specify the atomic positions [20]. Initially, the calculation of atomic scattering was done by considering 13 phase shifts ($l_{\max}=12$), whereas the final structural confirmation utilized 16 phase shifts ($l_{\max}=15$). Although the imaginary part of the inner potential (V_{oi}) was fixed to -5.0 eV, the real part was determined through theoretical–experimental fit. The best-fit model was obtained through best agreement between the experimental and theoretical $I(E)$ curves, which was decided by minimizing Pendry's reliability factor (R_p) [21]. The error bars on the structural parameters were calculated by variance of R_p, $\Delta R = R_{\min}(8|V_{oi}|/\Delta E)^{1/2}$, where $R_{\min}$ is the minimum R_p value and ΔE is the total energy range of the experimental $I(E)$ curves [21].

3. Results

3.1. $c(4\times4)$-3Pb

The $c(4\times4)$-Pb structure is obtained as a 1D arrangement of substitutional Pb atoms of coverage 0.375, which was first determined by Gauthier et al. [14]. Here, we have reconfirmed it more precisely with smaller R_p over a wider energy range. We will denote the structure as $c(4\times4)$-3Pb because there are three Pb atoms in the unit cell. Usually, a heavy metal on metal substrates does not show this kind of 1D structure. Therefore, we reexamined it by carrying out LEED $I(E)$ analysis with a total energy range of 5429 eV for 27 beams. We obtained a lower R_p value of 0.21, compared to 0.307 from the previous study [14]. The optimized Debye temperatures for Pb on the fourfold-hollow site and on the near-bridge site, as well for Cu atoms in the top layer, second layer, and bulk, were 110, 90, 260, 300, and 360 K, respectively. A comparison between calculated best-fit $I(E)$ curves and experimental ones is shown in Fig. 2, and the agreement is very good. The optimum structural parameters are given in Table 1.

Table 1
Optimal parameters of the best-fit structure for the $c(4\times4)$-3Pb phase. Atoms and their numbers are referenced in Fig. 6. The heights are calculated from the second complete Cu layer. Here, '0' represents no lateral displacement of the atoms in the specified direction due to symmetry requirement.

Atom No	Lateral displacement (Å)		Height (Å)
	[110]	$[\bar{1}10]$	
Pb2	0.77 ± 0.15	0	4.26 ± 0.07
Pb1	0	0	4.19 ± 0.05
Cu1	0	0	3.60 ± 0.02
Cu2	0	0.23 ± 0.13	3.62 ± 0.03
Cu3	0.04 ± 0.07	0.01 ± 0.07	1.86 ± 0.02
Cu4	0.01 ± 0.08	0.01 ± 0.06	1.76 ± 0.02

3.2. $c(4\times4)$-(2Pb, Bi) coadsorption

The coadsorption of Pb and Bi atoms is performed upon deposition of these two elements, one after the other at various coverages with monitoring of the LEED patterns. At first, Pb is deposited at a certain coverage; then, Bi is deposited onto the Pb pre-adsorbed surface, and LEED patterns are observed with gradual increase of Bi coverage. Within a total of two monolayers of coverage of Pb and Bi, the obtained phases $c(4\times4)$, $c(2\times2)$, and $c(9\sqrt{2}\times\sqrt{2})$ are shown in the surface phase diagram, as presented in Fig. 3. When the coadsorption was done in the opposite order, the same phase diagram was obtained.

The $c(4\times4)$ structure formed by coadsorption of Pb and Bi has been determined by tensor LEED analysis. Experimentally, we obtained this phase for Pb coverages of $0.1-0.4$ and Bi coverages of $0.3-0.1$, as shown in the phase diagram. For the theoretical calculation, we considered only a Pb coverage of 0.25 and a Bi coverage of 0.125, with a total adsorbate coverage of 0.375. We excluded other coverage combinations because we obtained the brightest LEED pattern under this condition. According to the coverage calculation of the $c(4\times4)$ unit cell, 0.375 corresponds to the three adsorbate atoms. Thus, there are two Pb atoms and one Bi atom in the unit cell, and the coverages of Pb and Bi are 2/8 and 1/8, respectively, which we denote as $c(4\times4)$-(2Pb, Bi). We have examined 12 structural models for $c(4\times4)$-(2Pb, Bi), as shown in Fig. 4. For the structural models we have considered fourfold-hollow sites and substitutional sites for the adsorption sites, and vacancies. The reason of our consideration is that, both atoms are located at substitutional sites in the Cu(001) for coverages lower than 0.5 and they move up on surface hollow sites at coverages of 0.5 or higher, as mentioned earlier. Among the 12 models, the first four are kept under *p4mm* symmetry, whereas the remaining eight correspond to the *p2mm* or *c2mm* symmetries. Models 1, 5, and 12 are overlayer structures; models 2 and 6 are substitutional structures. Models 7 and 11 are both substitutional and overlayer structures. Models 3, 4, and 8 are substitutional and vacancy structures in the top layer. Models 9 and 10 are substitutional, overlayer, and vacancy structures. All structures were optimized by minimizing R_p. The R_p values obtained by allowing relaxations in the first complete Cu substrate layer for each model are also shown in Fig. 4.